nature immunology

Cell-intrinsic lysosomal lipolysis is essential for alternative activation of macrophages

Stanley Ching-Cheng Huang[1], Bart Everts[1,6], Yulia Ivanova[1,6], David O'Sullivan[1,6], Marcia Nascimento[1], Amber M Smith[1], Wandy Beatty[2], Latisha Love-Gregory[3], Wing Y Lam[1], Christina M O'Neill[1], Cong Yan[4], Hong Du[4], Nada A Abumrad[3], Joseph F Urban Jr[5], Maxim N Artyomov[1], Erika L Pearce[1] & Edward J Pearce[1]

Alternative (M2) activation of macrophages driven via the α-chain of the receptor for interleukin 4 (IL-4Rα) is important for immunity to parasites, wound healing, the prevention of atherosclerosis and metabolic homeostasis. M2 polarization is dependent on fatty acid oxidation (FAO), but the source of the fatty acids that support this metabolic program has not been clear. We found that the uptake of triacylglycerol substrates via the scavenger receptor CD36 and their subsequent lipolysis by lysosomal acid lipase (LAL) was important for the engagement of elevated oxidative phosphorylation, enhanced spare respiratory capacity (SRC), prolonged survival and expression of genes that together define M2 activation. Inhibition of lipolysis suppressed M2 activation during infection with a parasitic helminth and blocked protective responses to this pathogen. Our findings delineate a critical role for cell-intrinsic lysosomal lipolysis in M2 activation.

Macrophages exist throughout the body as resident components of most tissues. They are embryonically derived, seeded into tissues *in utero* and maintained by *in situ* proliferation[1,2]. During inflammation, additional macrophages develop from monocytes recruited from the bone marrow[1] or from the proliferation of resident cells[3]. Macrophages are crucial for immunity and can adopt different activation states depending on the context. Interferon-γ (IFN-γ) in combination with agonists of Toll-like receptors promotes M1 (classical) activation, whereas the cytokines interleukin 4 (IL-4) and IL-13 promote M2 (alternative) activation[4,5]. From the host-defense standpoint, M1 macrophages are inflammatory and can serve a positive role in immunity to microbial pathogens and tumors[5]. In contrast, M2 macrophages promote tissue repair and metabolic homeostasis and serve key roles in immunity to parasitic helminths[5].

M1 and M2 macrophages have distinct metabolic phenotypes that differ from those of resting macrophages[6,7]. M1 macrophages rely on aerobic glycolysis, while M2 macrophages use fatty acid oxidation (FAO; also known as β-oxidation) to fuel mitochondrial oxidative phosphorylation. IL-4-induced changes in macrophage metabolism are dependent on the transcription factor STAT6 and are underpinned by induction of the expression of the nuclear receptor PPARγ coactivator PGC1β and associated mitochondrial biogenesis[8]. M2 activation is prevented by inhibition of FAO, whereas overexpression of PGC1β is sufficient to attenuate M1 activation in response to IFN-γ and lipopolysaccharide (LPS)[8]. Thus, IL-4-induced FAO is critical for M2 activation. In other cells of the immune system, FAO is known to support cellular longevity[9,10], but whether or not this is the case in macrophages is unclear.

Because of the health implications of the M2 activation of macrophages in various settings, there is considerable interest in understanding the cellular pathways that underpin the M2 phenotype. Despite the established importance of FAO for M2 activation, the source of the fatty acids that support this process is unknown. The consensus view from work with other cell types is that the fatty acids needed to meet metabolic and other requirements are released through a coordinated process of lipolysis from triacylglycerols stored in lipid droplets that is initiated by the enzyme adipose triglyceride lipase (ATGL)[11,12]. However, the expression of CD36, which is a receptor for the endocytosis of triacylglycerol-rich lipoprotein particles, such as LDL and VLDL[13,14], is induced in macrophages by IL-4 (ref. 15) and has been linked to M2 activation[16]. Such findings suggested to us that the uptake and lipolysis of exogenous triacylglycerols might serve to generate fatty acids for FAO in M2 macrophages. Consistent with this view, we report here that lysosomal lipolysis mediated by lysosomal acid lipase (LAL), an enzyme that is expressed in macrophages as they differentiate from monocytes[17] and is further induced by stimulation with IL-4, has an important role in M2 activation. Inhibition of this pathway suppressed changes in oxidative phosphorylation and macrophage longevity and the expression of key genes that mark commitment to M2 activation. Many of the effects of the inhibition of lipolysis were recapitulated in CD36-deficient macrophages. Our data highlight a previously unappreciated role for LAL in cell-intrinsic

[1]Department of Pathology and Immunology, Washington University School of Medicine, St. Louis, Missouri, USA. [2]Department of Molecular Microbiology, Washington University School of Medicine, St. Louis, Missouri, USA. [3]Department of Medicine and Cell Biology, Washington University School of Medicine, St. Louis, Missouri, USA. [4]Department of Pathology and Laboratory Medicine, Indiana University School of Medicine, Indiana, USA. [5]US Department of Agriculture, Agriculture Research Service, Beltsville Human Nutrition Research Center, Diet, Genomics and Immunology Laboratory, Beltsville, Maryland, USA. [6]These authors contributed equally to this work. Correspondence should be addressed to E.J.P. (edwardpearce@path.wustl.edu).

Received 1 March; accepted 2 July; published online 3 August 2014; doi:10.1038/ni.2956

lipolysis in macrophages to support FAO, show that this enzyme is integral to the M2 activation pathway and provide a framework for understanding the contribution of CD36 to these processes.

RESULTS

M2 activation depends on FAO

By extracellular flux analysis, we compared oxygen consumption by M0 (unactivated), M1 and M2 bone marrow–derived macrophages. We found that M2 macrophages had an enhanced mitochondrial oxygen-consumption rate (OCR) and markedly increased spare respiratory capacity (SRC; this is the quantitative difference between the maximal uncontrolled OCR and the initial basal OCR)[10,18] (**Fig. 1a**), indicative of increased commitment to oxidative phosphorylation. In contrast, we found no evidence of mitochondrial oxygen consumption in M1 macrophages (**Fig. 1a**), which relied instead on aerobic glycolysis, measured as the extracellular acidification rate (ECAR) (**Fig. 1b**), to meet their bioenergetic needs[19]. The extent of the metabolic difference between M1 cells and M2 cells was apparent in the overall ratio of oxidative phosphorylation to aerobic glycolysis, which was tenfold higher in M2 macrophages than in M1 macrophages (**Fig. 1c**), reflective of polar opposite core metabolic programs. Consistent with published reports[8,20], we found that the commitment of M2 macrophages to FAO and oxidative phosphorylation was evident in the increased expression of genes encoding molecules in these pathways (**Supplementary Fig. 1a**,**c**). This commitment was also sensitive to the suppression of mitochondrial oxygen consumption by etomoxir, an inhibitor of Cpt1, a key enzyme in FAO[8] (**Fig. 1d**). We found that etomoxir also eradicated SRC in M2 macrophages (**Fig. 1e**), which confirmed the link between FAO and heightened oxidative phosphorylation. Enhanced SRC has been linked to longevity in memory CD8$^+$ T cells[10]. We found such increased longevity also held true for macrophages, as M2 cells exhibited a substantial survival advantage over M0 and M1 cells in culture (**Supplementary Fig. 2**).

The activation of M2 macrophages and that of M1 macrophages are marked by differences in the expression of a large panel of genes, including *Mrc1* (which encodes the mannose receptor CD206), *Clec10a* (which encodes the C-type lectin CD301), *Retlna* (which encodes the effector RELMα), *Pdcd1lg2* (which encodes the ligand PD-L2) and *Nos2* (which encodes inducible nitric oxide synthase (iNOS)) (**Supplementary Fig. 1b**,**c**). By flow cytometry, we found that etomoxir substantially inhibited the expression of CD301, CD206 and RELMα in macrophages cultured in M2 conditions (**Fig. 1f**,**g**) but had comparatively little effect on the expression of iNOS in cells cultured in M1 conditions (**Fig. 1h**). Thus, FAO, measureable as increased baseline OCR and increased SRC, is essential for M2 activation.

Lipolysis contributes to M2 activation

The cellular requirements for fatty acids can be met by enzymatically regulated lipolysis of triacylglycerols into diacylglycerols and monoacylglycerols, accompanied by the release of fatty acids[11]; an endpoint of this process is the release of glycerol from cells in which lipolysis is occurring[11]. We used mass spectrometry for global metabolite profiling and found significantly greater amounts of three of four monoacylglycerols measured in M2 cells than in M1 cells (**Fig. 2a**), which indicated enhanced lipolysis in the M2 cells. Consistent with that conclusion, we found higher concentrations of extracellular glycerol in cultures of M2 macrophages than in those of M0 macrophages (**Fig. 2b**). To determine whether lipolysis is linked to FAO and oxidative phosphorylation, we stimulated cells with IL-4 in the presence or absence of tetrahydrolipistatin (orlistat), a clinically used,

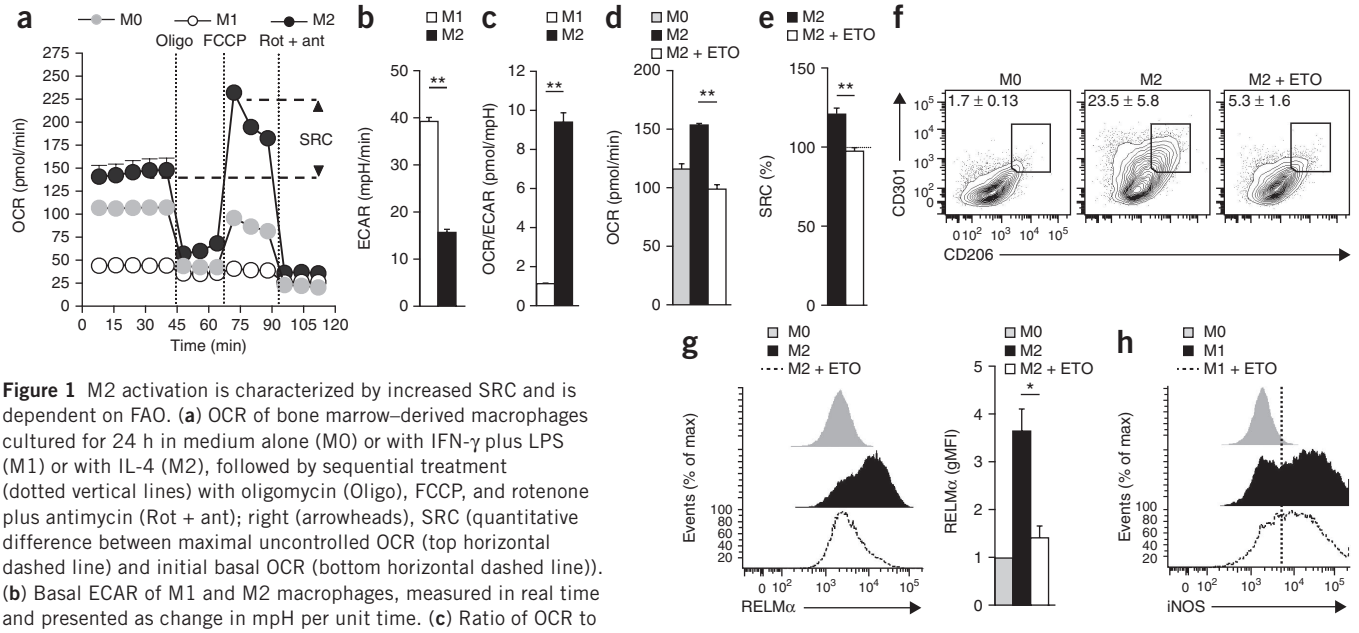

Figure 1 M2 activation is characterized by increased SRC and is dependent on FAO. (**a**) OCR of bone marrow–derived macrophages cultured for 24 h in medium alone (M0) or with IFN-γ plus LPS (M1) or with IL-4 (M2), followed by sequential treatment (dotted vertical lines) with oligomycin (Oligo), FCCP, and rotenone plus antimycin (Rot + ant); right (arrowheads), SRC (quantitative difference between maximal uncontrolled OCR (top horizontal dashed line) and initial basal OCR (bottom horizontal dashed line)). (**b**) Basal ECAR of M1 and M2 macrophages, measured in real time and presented as change in mpH per unit time. (**c**) Ratio of OCR to ECAR for M1 and M2 macrophages. (**d**) Basal OCR of M0 and M2 macrophages and OCR of M2 macrophages treated with etomoxir (M2 + ETO). (**e**) SRC of M2 macrophages left untreated (M2) or treated with etomoxir (M2 + ETO). (**f**) Expression of CD301 and CD206 on untreated M0 macrophages and M2 macrophages left untreated or treated with etomoxir, assessed by flow cytometry. Numbers adjacent to outlined areas indicate percent CD301$^+$CD206$^+$ cells (mean ± s.e.m.). (**g**) RELMα expression by macrophages as in **f**. Right, geometric mean fluorescence intensity (gMFI) of RELMα, relative to that of M0 macrophages, set as 1. (**h**) iNOS expression by macrophages cultured for 24 h in nonpolarizing (M0) or M1-polarizing conditions in the presence or absence of etomoxir (key). iNOS$^+$ cells (mean ± s.e.m.): 69.7% ± 1.3% (M1) or 60.5% ± 9.7% (M1 plus ETO). *$P < 0.05$ and **$P < 0.0001$ (Student's *t*-test). Data are from one experiment representative of more than three independent experiments (**a**–**e**; mean and s.e.m. (**a**) or mean and s.e.m. of five or more technical replicates (**b**–**e**)), one experiment representative of two experiments (**f**,**h**; mean ± s.e.m. of both) or one experiment representative of three experiments (**g**, left) or are from three independent experiments (**g**, right; mean and s.e.m.).

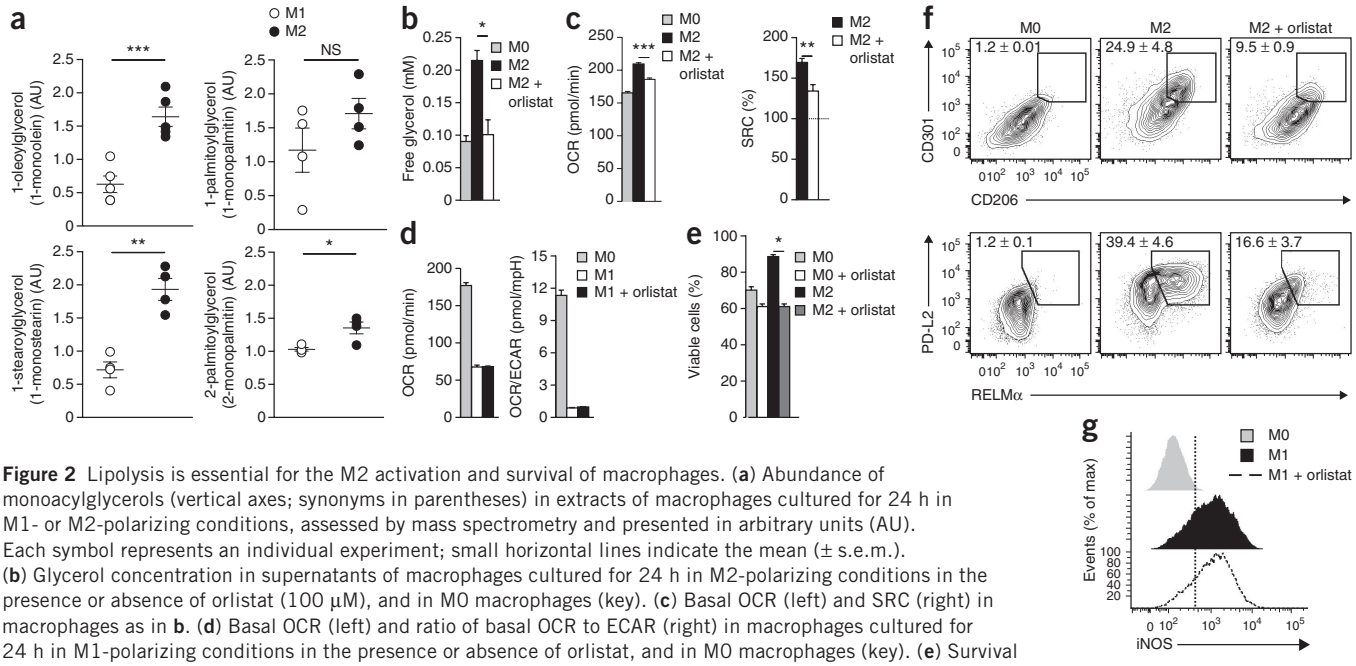

Figure 2 Lipolysis is essential for the M2 activation and survival of macrophages. (**a**) Abundance of monoacylglycerols (vertical axes; synonyms in parentheses) in extracts of macrophages cultured for 24 h in M1- or M2-polarizing conditions, assessed by mass spectrometry and presented in arbitrary units (AU). Each symbol represents an individual experiment; small horizontal lines indicate the mean (± s.e.m.). (**b**) Glycerol concentration in supernatants of macrophages cultured for 24 h in M2-polarizing conditions in the presence or absence of orlistat (100 μM), and in M0 macrophages (key). (**c**) Basal OCR (left) and SRC (right) in macrophages as in **b**. (**d**) Basal OCR (left) and ratio of basal OCR to ECAR (right) in macrophages cultured for 24 h in M1-polarizing conditions in the presence or absence of orlistat, and in M0 macrophages (key). (**e**) Survival of macrophages cultured for 48 h in nonpolarizing (M0) or M2-polarizing conditions in the presence or absence of orlistat. (**f**) Expression of CD301 and CD206 (top) and of PD-L2 and RELMα (bottom) by macrophages as in **b**, assessed by flow cytometry. Numbers adjacent to outlined areas indicate percent CD301$^+$CD206$^+$ cells (top) or PD-L2$^+$RELMα$^+$ cells (bottom) (mean ± s.e.m.). (**g**) iNOS expression in macrophages as in **d**. iNOS$^+$ cells (mean ± s.e.m.): 68.2% ± 5.0% (M1) and 70.2% ± 6.7% (M1 plus orlistat). NS, not significant; $^*P < 0.05$, $^{**}P < 0.01$ and $^{***}P < 0.0001$ (Student's *t*-test). Data are from four independent experiments (**a**), one experiment representative of three experiments (**b**–**e**; mean and s.e.m. of three technical replicates) or one experiment representative of two experiments (**f**,**g**; mean ± s.e.m. of both).

active site–directed lipase inhibitor[21]. We found that orlistat inhibited IL-4-induced increases in lipolysis, as measured by glycerol production (**Fig. 2b**), and suppressed the associated changes in oxidative phosphorylation (**Fig. 2c**), although it had no effect on the metabolic changes induced by M1 conditions (**Fig. 2d**). These reductions in oxidative phosphorylation and SRC in orlistat-treated M2 cells were linked to significantly lower survival, evident as their decreased viability by day 2 of culture (**Fig. 2e**). Orlistat had less marked effects on the survival of M0 cells (**Fig. 2e**). Within the short time frame that M1 cells remained alive, we detected no substantial effect of inhibiting lipolysis on their survival (data not shown). Given the close link between FAO and M2 activation, we next assessed the effect of inhibiting lipolysis on macrophages stimulated with IL-4. We found that orlistat suppressed the IL-4-induced expression of CD206, CD301, PD-L2 and RELMα (**Fig. 2f**) but had no effect on iNOS expression in M1 macrophages (**Fig. 2g**). Together these data indicated that lipolysis supported FAO and in this way was critical for M2 activation.

LAL is responsible for lipolysis upstream of FAO

Our data indicated lipolysis was a critical mechanism for the generation of fatty acids for FAO and the M2 activation of macrophages stimulated with IL-4. In other cells, fatty acids for FAO are released from triacylglycerols stored in lipid droplets with cholesterol esters by a process of lipolysis that is initiated by ATGL and is continued by hormone-sensitive lipase, encoded by *Pnpla2* and *Lipe*, respectively[11,12,22]. However, among genes encoding lipases, we found that *Pnpla2* and *Lipe* had higher expression in M1 cells than in M2 cells (**Fig. 3a**), which suggested that the lipases encoded by these genes might not be involved in M2 activation. To directly test this, we measured RELMα expression in peritoneal macrophages from *Pnpla2*$^{-/-}$ mice following intraperitoneal injection of complexes of IL-4 and antibody to IL-4 (IL-4c), a procedure shown previously to induce the M2 activation of peritoneal macrophages[23]. We found that >90% of macrophages in *Pnpla2*$^{-/-}$ mice or wild-type mice expressed RELMα following injection of IL-4c (**Supplementary Fig. 3a**), which indicated that the loss of ATGL had no effect on M2 activation. A substantial body of literature has associated M1 activation with the development of lipid droplets[24], but whether or not lipid droplets are prevalent in M2 macrophages has remained unclear. By transmission electron microscopy, we found that M1 macrophages contained easily identifiable lipid droplets, whereas M2 cells did not (**Fig. 3b**). Together with the lipase-expression data and data from experiments with *Pnpla2*$^{-/-}$ macrophages, these findings suggested that M2 macrophages were not using canonical lipid droplet–triacylglycerol hydrolysis pathways to generate fatty acids for FAO. Nevertheless, we did observe that neutral lipids (assessed by staining with the fluorescent dye BODIPY, detected by flow cytometry), lipid droplets (visualized by electron microscopy) and triacylglycerols and cholesterol esters (quantified by mass spectrometry) accumulated in macrophages stimulated with IL-4 in the presence of orlistat (**Supplementary Fig. 3b–d**). Mass spectrometry additionally confirmed that neutral lipid stores were larger in M1 macrophages than in M2 macrophages (**Supplementary Fig. 3d**). These findings indicated that M2 macrophages accumulated neutral lipid stores when lipolysis was inhibited.

We noted that unlike the expression of genes encoding many other cellular lipases (including *Pnpla2*, *Lipe*, *Lipc* and *Lipg*), expression of *Lipa* was upregulated in M2 macrophages relative to its expression in M1 macrophages (**Fig. 3a** and **Supplementary Fig. 1c**), which suggested that its product might be important for M2 activation. *Lipa* encodes LAL, a triacylglycerol lipase that is able to break down triacylglycerols delivered into the lysosomes by endocytosis of low-density lipoproteins (LDLs and VLDLs)[25]. Since LAL is a known target of orlistat[26], we reasoned that the effects of orlistat on the FAO and M2 activation of macrophages we had observed (**Fig. 2**) might

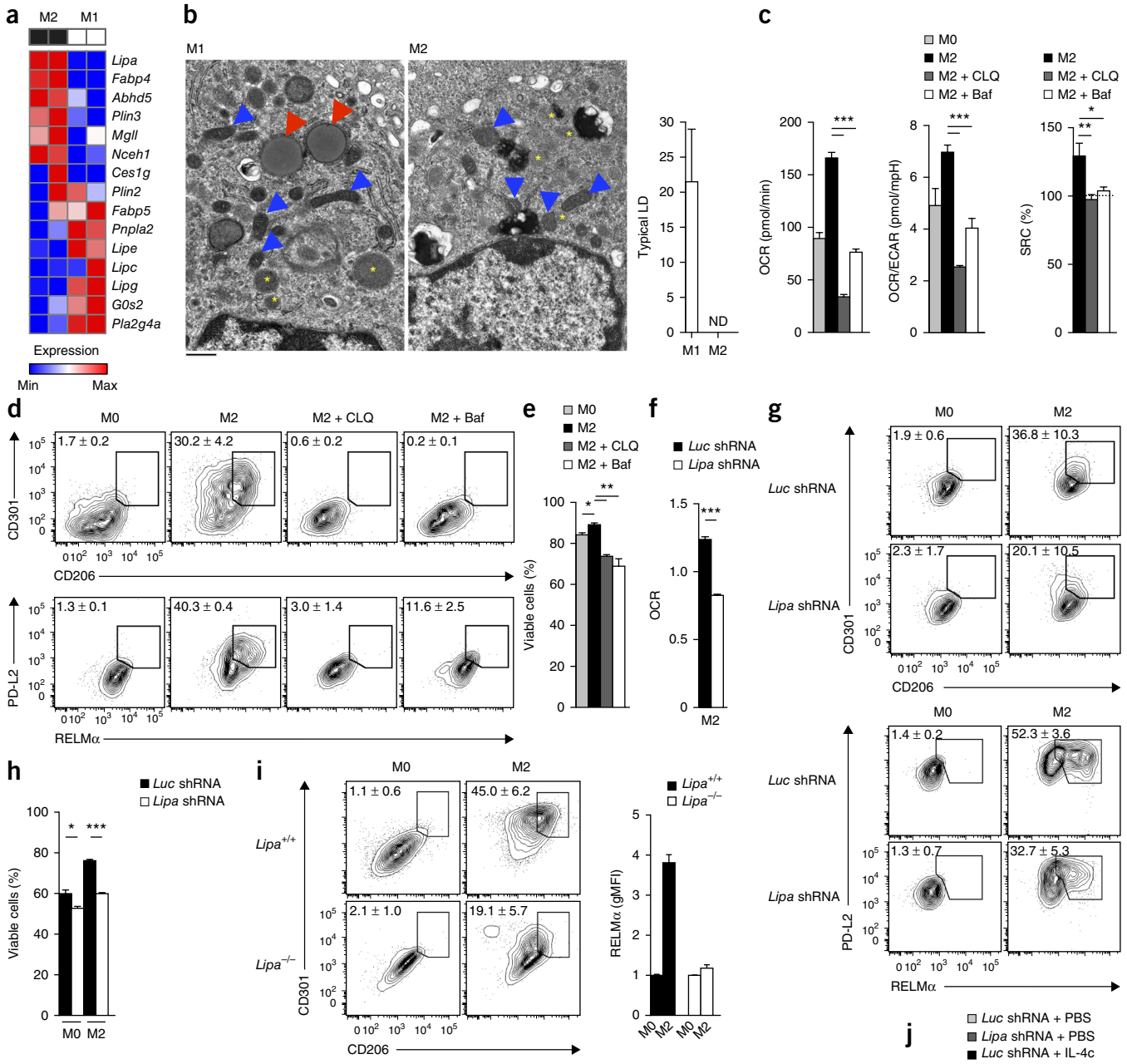

Figure 3 Lipolysis for M2 activation is mediated by LAL. (**a**) Expression of genes encoding molecules involved in lipolysis (right margin) in M2 and M1 macrophages, assessed by high-throughput sequencing of RNA. (**b**) Transmission electron microscopy (left) of bone marrow–derived M1 and M2 macrophages, showing mitochondria (blue arrowheads), lysosomes (yellow asterisks) and lipid droplets (red arrowheads), and quantification of lipid droplets (LD) per cell ($n \geq 150$ cells per condition). ND, not detected. Scale bar (left), 500 nm. (**c**) Basal OCR (left), ratio of OCR to ECAR (middle) and SRC (right) of M2 macrophages left untreated or treated with chloroquine (CLQ) or bafilomycin (Baf), and of untreated M0 macrophages (key). (**d**) Expression of CD301 and CD206 (top) and of PD-L2 and RELMα (bottom) by macrophages as in **c**, assessed by flow cytometry (numbers in plots, as in **Fig. 2f**). (**e**) Viability of M0 and M2 macrophages cultured for 24 h in the presence or absence of chloroquine or bafilomycin (key). (**f**) Basal OCR of M2 macrophages transduced with control virus (*Luc* shRNA) or virus expressing shRNA directed against *Lipa* (*Lipa* shRNA); results are presented relative to those of untransduced M0 macrophages. (**g**) Expression of CD301 and CD206 (top) and of PD-L2 and of RELMα (bottom) by macrophages transduced with shRNA as in **f** (numbers in plots, as in **Fig. 2f**). (**h**) Viability of macrophages transduced with shRNA as in **f** and then cultured for 2 d in nonpolarizing (M0) or M2-polarizing conditions. (**i**) Expression of CD301 and CD206 (left) and of RELMα (right) by $Lipa^{+/+}$ or $Lipa^{-/-}$ M0 or M2 macrophages (numbers in plots, as in **Fig. 2f**). (**j**) Frequency of RELMα$^+$ peritoneal macrophages in chimeras reconstituted with bone marrow transduced with retrovirus expressing control or *Lipa*-specific shRNA (as in **f**) and a human CD8 reporter (huCD8$^+$), followed by injection of the chimeras with PBS or IL-4c (left), as well as of unstransduced (huCD8$^-$) peritoneal macrophages from the same mice (right). NS, not significant; $^*P < 0.05$, $^{**}P < 0.01$ and $^{***}P < 0.0001$ (Student's *t*-test). Data are from two independent experiments (**a**,**b**; mean and s.e.m. in **b**, right), one experiment representative of three experiments (**c**,**e**,**f**; mean and s.e.m. of three technical replicates), one experiment representative experiment of two experiments (**d**,**g**,**i**; mean ± s.e.m. of both), two to three independent experiments (**h**,**i**; mean and s.e.m.) or one experiment (**j**; mean and s.e.m. of at least two mice).

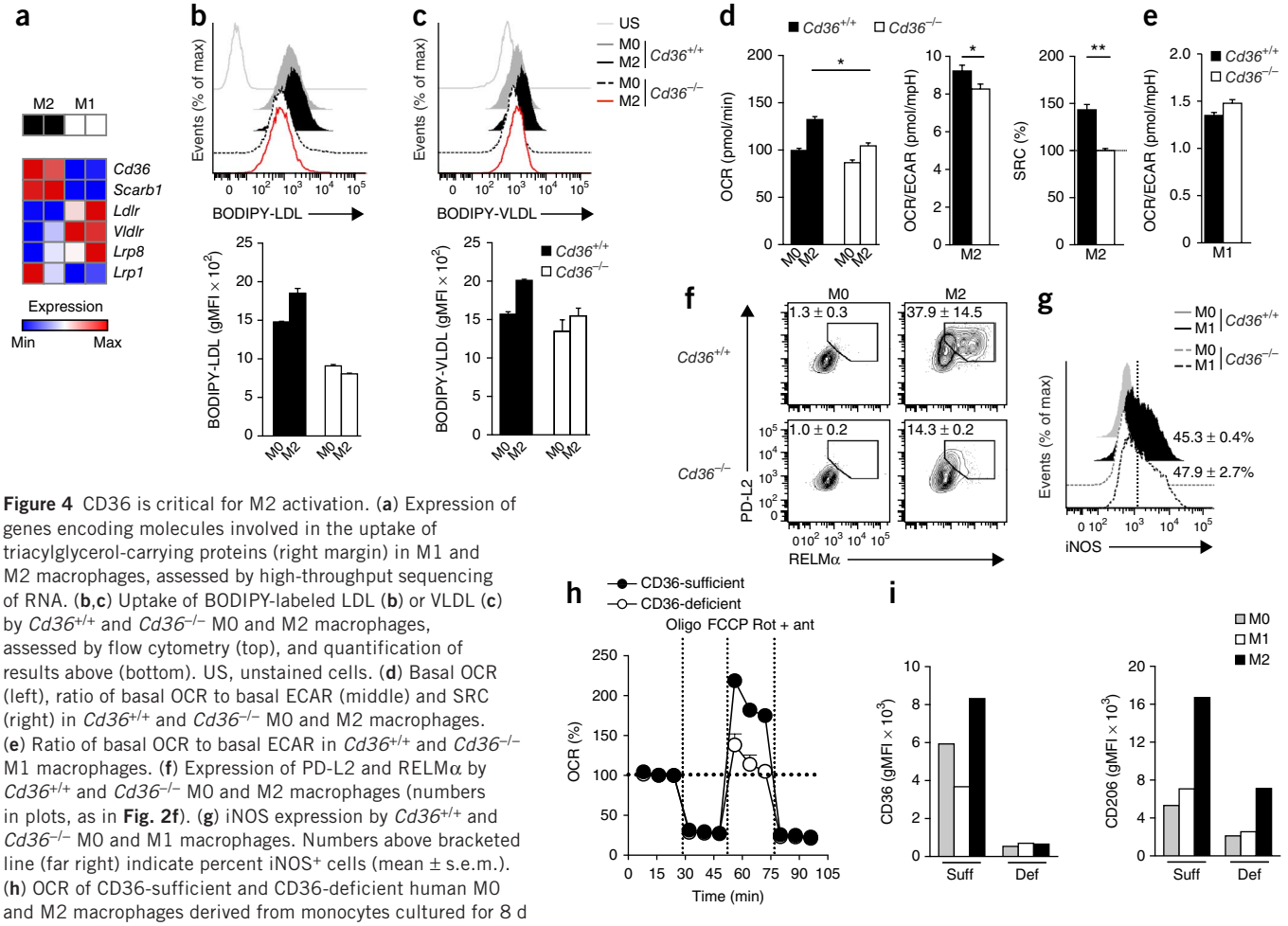

Figure 4 CD36 is critical for M2 activation. (**a**) Expression of genes encoding molecules involved in the uptake of triacylglycerol-carrying proteins (right margin) in M1 and M2 macrophages, assessed by high-throughput sequencing of RNA. (**b**,**c**) Uptake of BODIPY-labeled LDL (**b**) or VLDL (**c**) by *Cd36*$^{+/+}$ and *Cd36*$^{-/-}$ M0 and M2 macrophages, assessed by flow cytometry (top), and quantification of results above (bottom). US, unstained cells. (**d**) Basal OCR (left), ratio of basal OCR to basal ECAR (middle) and SRC (right) in *Cd36*$^{+/+}$ and *Cd36*$^{-/-}$ M0 and M2 macrophages. (**e**) Ratio of basal OCR to basal ECAR in *Cd36*$^{+/+}$ and *Cd36*$^{-/-}$ M1 macrophages. (**f**) Expression of PD-L2 and RELMα by *Cd36*$^{+/+}$ and *Cd36*$^{-/-}$ M0 and M2 macrophages (numbers in plots, as in **Fig. 2f**). (**g**) iNOS expression by *Cd36*$^{+/+}$ and *Cd36*$^{-/-}$ M0 and M1 macrophages. Numbers above bracketed line (far right) indicate percent iNOS^{+} cells (mean ± s.e.m.). (**h**) OCR of CD36-sufficient and CD36-deficient human M0 and M2 macrophages derived from monocytes cultured for 8 d in macrophage colony-stimulating factor, assessed before and after sequential treatment with oligomycin, FCCP, and rotenone and antimycin A; results are presented relative to basal OCR before treatment (dotted horizontal line), set as 100%. (**i**) Expression of CD36 and CD206 in CD36-sufficient (Suff) and CD36-deficient (Def) human M0, M1 and M2 monocyte-derived macrophages. *$P < 0.01$ and **$P < 0.0001$ (Student's *t*-test). Data are from two independent experiments (**a**, and **b**,**c**, bottom; mean ± s.e.m. in **b**,**c**), one experiment representative of two experiments (**b**,**c**, top, and **f**,**g**; mean ± s.e.m. of both in **f**,**g**), one experiment representative of two independent experiments (**d**,**e**; mean ± s.e.m. of three technical replicates) or one experiment with one donor per genotype (**h**,**i**; mean and s.e.m. of at least four technical replicates in **h**).

reflect inhibition of LAL function in this system. To investigate the role of LAL (which, unlike the other cellular lipases, has optimal activity at an acidic pH rather than at a neutral pH) in M2 activation, we first neutralized lysosomal pH with chloroquine or bafilomycin A1. We found that these conditions completely inhibited the IL-4-induced increases in oxidative phosphorylation, as measured by OCR, the OCR/ECAR ratio and SRC (**Fig. 3c**). These effects were accompanied by inhibition of the IL-4-induced increases in the expression of CD206, CD301, PD-L2 and RELMα (**Fig. 3d**) and a decrease in longevity (**Fig. 3e**). These data supported the view that an acidic compartment was essential for M2 activation and were consistent with the proposal of a role for LAL in this process. To formally address this possibility, we targeted LAL with short hairpin RNA (shRNA) and found that increased oxidative phosphorylation, higher expression of CD206, CD301, RELMα and PD-L2 and increased longevity in response to IL-4 were significantly inhibited by the suppression of LAL expression (**Fig. 3f–h**). Suppression of LAL expression also resulted in the accumulation of lipid droplets in macrophages stimulated with IL-4 (**Supplementary Fig. 3b**). Additionally, we examined the ability of *Lipa*$^{-/-}$ macrophages to become M2 activated and found that increases in the expression of CD206, CD301 and RELMα were substantially attenuated in *Lipa*$^{-/-}$ macrophages relative to those in *Lipa*$^{+/+}$ cells (**Fig. 3i**). Finally, we made bone marrow chimeras by reconstituting irradiated CD45.2^{+} mice with CD45.1^{+} bone marrow that had been transduced with retrovirus encoding shRNA targeting *Lipa* or a control gene (encoding luciferase). We were able to distinguish the progeny of transduced cells by the expression of human coreceptor CD8 encoded as a reporter by the retrovirus. We examined the M2 activation of peritoneal macrophages derived from transduced CD45.1^{+} bone marrow cells and of those derived from their untransduced counterparts, following intraperitoneal injection of IL-4c into the host mice. We found that the RELMα expression of peritoneal macrophages in response to IL-4 was inhibited by the suppression of LAL expression (**Fig. 3j**). Together these data indicated a critical role for cell-intrinsic lipolysis mediated by LAL in optimal M2 activation of macrophages in response to IL-4.

Optimal M2 activation depends on CD36

The importance of LAL in M2 macrophages suggested that the delivery of triacylglycerol to lysosomes is a key process in the generation of fatty acids to support FAO and M2 activation. We examined the expression of receptors that mediate the uptake of triacylglycerol-carrying

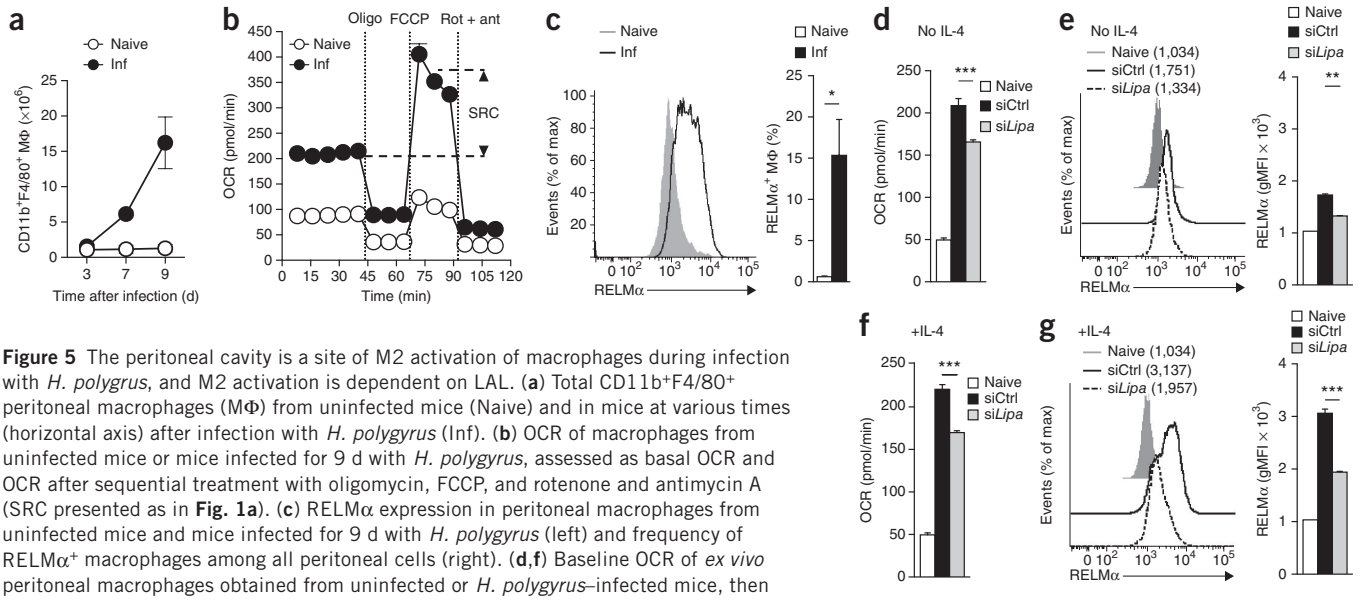

Figure 5 The peritoneal cavity is a site of M2 activation of macrophages during infection with *H. polygyrus*, and M2 activation is dependent on LAL. (**a**) Total CD11b$^+$F4/80$^+$ peritoneal macrophages (MΦ) from uninfected mice (Naive) and in mice at various times (horizontal axis) after infection with *H. polygyrus* (Inf). (**b**) OCR of macrophages from uninfected mice or mice infected for 9 d with *H. polygyrus*, assessed as basal OCR and OCR after sequential treatment with oligomycin, FCCP, and rotenone and antimycin A (SRC presented as in **Fig. 1a**). (**c**) RELMα expression in peritoneal macrophages from uninfected mice and mice infected for 9 d with *H. polygyrus* (left) and frequency of RELMα$^+$ macrophages among all peritoneal cells (right). (**d**,**f**) Baseline OCR of *ex vivo* peritoneal macrophages obtained from uninfected or *H. polygyrus*–infected mice, then treated with nontargeting control siRNA (siCtrl) or *Lipa*-specific siRNA (si*Lipa*) and cultured for 12 h in the absence (**d**) or presence (**f**) of IL-4. (**e**,**g**) RELMα expression by the macrophages in **d** (**e**) and **f** (**g**). $^*P < 0.05$, $^{**}P < 0.001$ and $^{***}P < 0.0001$ (Student's *t*-test). Numbers in parentheses (left) indicate mean fluorescence intensity. Data are one experiment representative of three experiments (**a**–**c**; mean ± s.e.m. of two to four mice (**a**) or five technical replicates of two to four mice per group (**b**) or two to three mice per group (**c**, right) or with cells pooled from two mice (**c**, left)) or one experiment representative of two experiments (**d**,**f**,**g**; mean and s.e.m. of three technical replicates for cells pooled from two mice per group (**d**,**f**) or two mice per group (**g**)) or are representative of two experiments with one mouse representative of two mice per group (**e**; mean and s.e.m.).

serum lipoproteins in M2 macrophages and observed that CD36 expression was upregulated in M2 cells[15] (**Fig. 4a**). The same was true for *Scarb1* (which encodes the related scavenger receptor SR-B1) but not for *Ldlr1*, *Vldlr* or *Lrp8* (**Fig. 4a** and **Supplementary Fig. 1c**). On the basis of these observations, and the fact that CD36 has been linked to M2 activation[16], we hypothesized that CD36 might serve a role in the increased FAO in M2 macrophages by facilitating the uptake of triacylglycerols. To investigate this, we assessed the responses to IL-4 of macrophages made from the bone marrow of *Cd36*$^{-/-}$ mice. We found that *Cd36*$^{+/+}$ M2 macrophages took up more LDL (**Fig. 4b**) and VLDL (**Fig. 4c**) than M0 macrophages did, but *Cd36*$^{-/-}$ M2 macrophages did not. In addition to being a receptor for LDL and VLDL, CD36 is a fatty acid translocase[13,14]. While we found M2 macrophages were more able to take up palmitate than were M0 cells, we observed no difference between *Cd36*$^{+/+}$ and *Cd36*$^{-/-}$ cells in this uptake (**Supplementary Fig. 4a**), which suggested that the fatty acid–translocase activity of CD36 did not account for the increased uptake of free fatty acids by M2 cells. *Cd36*$^{-/-}$ macrophages exhibited significantly lower IL-4-induced increases in oxidative phosphorylation than those of *Cd36*$^{+/+}$ macrophages, as measured by OCR, the OCR/ECAR ratio and SRC (**Fig. 4d**), but were substantially similar in terms of the metabolic markers of M1 activation (**Fig. 4e**). Consistent with a critical role for FAO in M2 activation, *Cd36*$^{-/-}$ macrophages had much lower expression of PD-L2 and RELMα in response to IL-4 than did *Cd36*$^{+/+}$ macrophages (**Fig. 4f**). In contrast, iNOS expression was similar in *Cd36*$^{+/+}$ and *Cd36*$^{-/-}$ macrophages stimulated in M1 conditions (**Fig. 4g**). We further addressed the role of CD36 by inhibiting CD36 in wild-type macrophages with sulfo-*N*-succinimidyl oleate (SSO) and examining the effect of this inhibition on responses to IL-4 (ref. 27). The findings of these experiments confirmed those of our studies with *Cd36*$^{-/-}$ macrophages. We found that LDL uptake was substantially inhibited by SSO (**Supplementary Fig. 4b**). Moreover, SSO completely blocked IL-4-induced increases in oxidative phosphorylation, as measured by OCR, the OCR/ECAR ratio and SRC (**Supplementary Fig. 4c**), but had no effect on metabolic markers of M1 activation (**Supplementary Fig. 4d**). SSO substantially inhibited the expression of CD206, CD301, PD-L2 and RELMα in response to IL-4 (**Supplementary Fig. 4e**) but had no effect on iNOS expression in M1 macrophages (**Supplementary Fig. 4f**). Together these data supported the view that elevated CD36 expression in macrophages in response to IL-4 had an important role in increased uptake of LDL and VLDL and that this pathway supported FAO and M2 activation.

Next we assessed the ability of monocyte-derived macrophages from a CD36-deficient patient to become alternatively activated in response to IL-4. We found that SRC was substantially diminished in CD36-deficient human M2 macrophages compared with that in CD36-sufficient human M2 macrophages (**Fig. 4h**). Expression of CD206 (the mannose receptor MRC1) is a marker of human M2 activation, as is expression of CD36 (ref. 28). Thus, we used flow cytometry to examine the expression of CD36 and CD206 in M0, M1 and M2 macrophages from CD36-sufficient and CD36-deficient subjects. We found higher expression of CD36 and CD206 in M2 macrophages than in M0 or M1 macrophages and much lower expression of CD206 in CD36-deficient macrophages stimulated with IL-4 than in their CD36-sufficient counterparts (**Fig. 4i**). Together with our findings from mouse *Cd36*$^{-/-}$ macrophages and the SSO-inhibitor studies, these data from human CD36-deficient macrophages supported the proposal of a role for CD36 in M2 activation.

Our data suggested that the lysosomal lipolysis of exogenous triacylglycerols acquired through a CD36-dependent mechanism was important for optimal M2 activation. Thus, we reasoned that depriving macrophages of exogenous triacylglycerols should affect M2 activation. We cultured macrophages for 24 h in complete medium containing or lacking serum, stimulated the cells for an additional 24 h with IL-4 and measured the expression of genes encoding key M2 markers. In these experiments, M2 activation was substantially inhibited, but not prevented, by the absence of serum (**Supplementary Fig. 5a**).

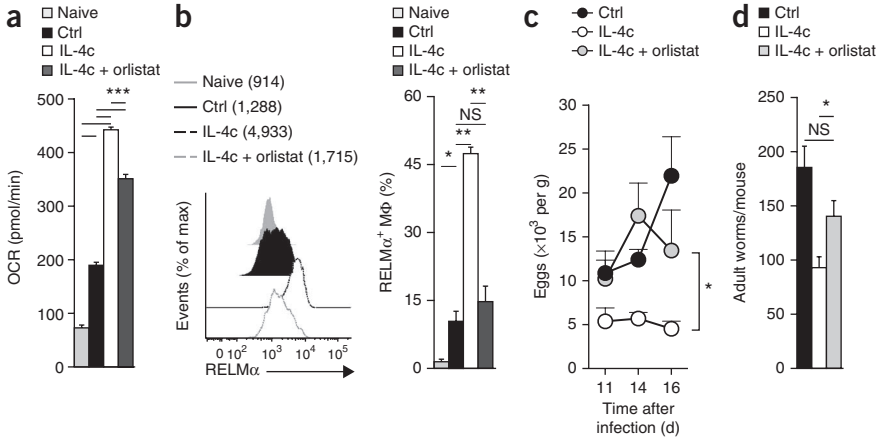

Figure 6 Inhibition of lipolysis suppresses IL-4-driven M2 activation of macrophages *in vivo* and the elimination of a primary *H. polygyrus* infection. (**a**) Basal OCR of peritoneal macrophages isolated from mice left uninfected and untreated (Naive) or from mice infected with *H. polygyrus* and, 9 d later, given injection of PBS (Ctrl), IL-4c or IL-4c plus orlistat (key), with injection of IL-4c again on day 14 after infection and treatment with orlistat repeated on days 11, 14 and 16 after infection, followed by analysis on day 17 after infection. (**b**) RELMα expression by peritoneal macrophages from mice as in **a** (left) and frequency of RELMα$^+$ macrophages (right). Numbers in parentheses (left) indicate mean fluorescence intensity. (**c**) Fecal egg counts over time in mice infected and treated as in **a**. (**d**) Adult worm counts at day 17 in mice infected and treated as in **a**. $^*P < 0.05$, $^{**}P < 0.001$ and $^{***}P < 0.0001$ (Student's *t*-test). Data are from one experiment representative of two experiments (mean and s.e.m. of five technical replicates of cells from three to six mice per group (**a**) or of three to six mice per group (**b**, right, **c**,**d**), or one mouse per group representative of three to six mice per group (**b**, left)).

Consistent with our data indicating the involvement of CD36-mediated uptake of LDL and VLDL in M2 macrophages, we found that under serum-free conditions, M2 activation was promoted by the addition of LDL and VLDL (**Supplementary Fig. 5a**). The finding that M2 activation was able to proceed to some extent in the absence of serum suggested that macrophages have an alternative pathway for fueling FAO. A candidate for such an alternative pathway is fatty acid synthesis. To explore this possibility, we examined how M2 activation was affected by TOFA, an inhibitor of acetyl-CoA carboxylase that catalyzes an early step in the synthesis of fatty acids from acetyl-CoA. TOFA completely blocked M2 activation in serum-free conditions and, in the presence of serum, reduced activation to levels observed in inhibitor-free, serum-free conditions (**Supplementary Fig. 5b**). These data suggested that macrophages have an underlying pathway through which, in the presence of IL-4, they synthesize fatty acids to support M2 activation, and that optimal M2 activation requires contributions of exogenous triacylglycerols and newly synthesized fatty acids.

The findings reported above raised the question of whether M2 macrophages first incorporate endogenously synthesized fatty acids into triacylglycerols before liberating them by lipolysis for FAO, which has been suggested to be the dominant pathway in other cell types[11]. We examined this by first assessing the effect of orlistat on M2 activation in serum-free conditions. We found that the inhibition of lipolysis under these conditions did inhibit M2 activation (**Supplementary Fig. 5b**), which indicated that endogenously synthesized fatty acids were incorporated into triacylglycerols in M2 macrophages. Triacylglycerols synthesized in this way are stored as lipid droplets, but our ultrastructural analysis did not identify lipid droplets in M2 cells (**Fig. 3b**). However, we did observe lipid droplets in macrophages stimulated with IL-4 in the presence of orlistat and in macrophages transduced with shRNA targeting *Lipa* (**Supplementary Fig. 3b**). Since the inhibition of lipolysis precludes the synthesis of these neutral lipid stores from fatty acids liberated from acquired triacylglycerols, we assumed that they were produced from newly synthesized fatty acids. Together our data raised the possibility that in addition to a primary pathway in which exogenous triacylglycerols were broken down in the lysosomal compartment to support FAO, M2 macrophages were also able to synthesize triacylglycerols from newly synthesized fatty acids and hydrolyze these via the same pathway.

M2 activation during helminth infection is LAL dependent

Our data indicated that lipolysis was essential for the metabolic switch and associated changes in the expression of key genes that occurred as macrophages became alternatively activated in response to IL-4. To assess whether lipolysis was critical for M2 activation *in vivo*, we used the *Heligmosomoides polygyrus bakeri* (*H. polygyrus*) mouse model of human intestinal helminth infection, in which M2 macrophages have an essential role in immunity[29]. We found that the number of peritoneal macrophages increased significantly over time during this infection (**Fig. 5a**) and that peritoneal macrophages from infected mice exhibited the metabolic profile of IL-4-activated bone marrow macrophages, with heightened baseline OCR and considerable SRC (**Fig. 5b**). Consistent with published observations[30], a substantial frequency of peritoneal macrophages from *H. polygyrus*–infected mice expressed the M2 marker RELMα (**Fig. 5c**). We found that maintenance of the M2-activation phenotype of peritoneal macrophages was dependent on LAL in this setting, since increases in OCR and RELMα expression were significantly inhibited in peritoneal macrophages treated *ex vivo* with small interfering RNA (siRNA) targeting *Lipa* (**Fig. 5d**,**e**). The dependence of M2 activation on LAL was also apparent in peritoneal cells maintained in a type 2 environment through the addition of IL-4 *in vitro* (**Fig. 5f**,**g**). These data indicated that macrophages in a type 2 cytokine environment *in vivo* exhibited lipolysis-dependent changes in metabolism and expression of genes encoding M2 markers equivalent to those induced by IL-4 in bone marrow–derived macrophages *in vitro*.

Inhibition of lipolysis suppresses parasite elimination

Primary infection of C57BL/6 mice with *H. polygyrus* is chronic despite the development of a type 2 cytokine response. However, injection of IL-4c into infected mice results in a reduction in the number of adult parasites, and M2 macrophages have been linked to the protective mechanism induced by this cytokine[3,29,31]. Given our findings, we reasoned that lipolysis should be crucial for the development of M2 macrophages in these settings and therefore that inhibition of this pathway would limit the expression of M2 macrophage–dependent protective immune responses. We found that injection of IL-4c after primary infection markedly enhanced the oxidative phosphorylation of peritoneal macrophages (**Fig. 6a**) and their RELMα expression (**Fig. 6b**) while simultaneously significantly reducing parasite burden, as measured by quantification of eggs and adult worms (**Fig. 6c**,**d**).

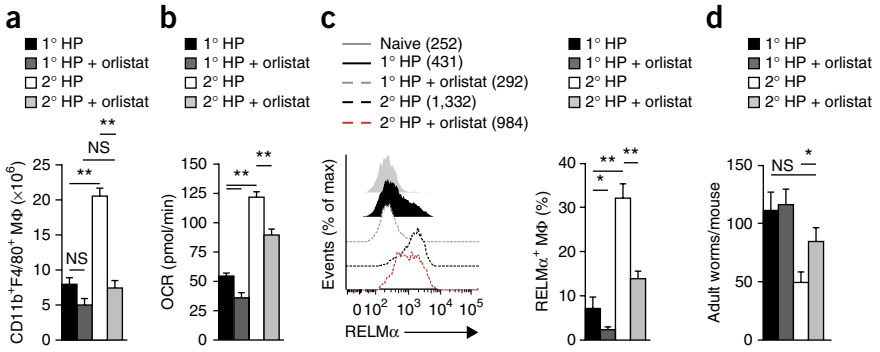

Figure 7 Inhibition of lipolysis suppresses resistance to reinfection with *H. polygyrus*. (**a**) Quantification of CD11b$^+$F4/80$^+$ peritoneal macrophages from mice infected with *H. polygyrus* and treated with pyrantel pamoate, followed by secondary infection with *H. polygyrus* (2° HP), or from mice infected for the first time with *H. polygyrus* at the time of the secondary infection of the other group (1° HP), with no additional treatment or treatment with orlistat (key) on the day of infection and on days 2, 4, 6 and 8 after infection, analyzed on day 9 after infection. (**b**) Basal OCR of peritoneal macrophages from mice treated as in **a**. (**c**) RELMα expression by peritoneal macrophages from mice treated as in **a** (presented as in **Fig. 6b**). (**d**) Adult worm counts in mice treated as in **a**. NS, not significant; $*P < 0.05$ and $**P < 0.0001$ (Student's *t*-test). Data are from one experiment representative of two experiments (mean and s.e.m. of four to ten mice per group (**a**,**c**, right, **d**), five technical replicates from cells of four to eight or more mice per group (**b**) or five to eight mice per group (**d**), or from one mouse representative of three to eight mice per group (**c**, left)).

Consistent with the proposal of a major role for lipolysis in M2 polarization, we found that the enhanced M2 activation and concomitant protective effects associated with the injection of IL-4c were significantly inhibited by parenteral treatment with orlistat (**Fig. 6**).

Mice in which primary *H. polygyrus* is cleared by chemotherapy exhibit a degree of immunity to secondary infection[29]. We compared the response of peritoneal macrophages during primary *H. polygyrus* infection with their response to a secondary infection after mice had cleared the parasite via administration of the anti-helminthic pyrantel pamoate and had been allowed to 'rest' for 5 weeks. We found that the number of peritoneal macrophages (**Fig. 7a**) and the magnitude of the increase in oxidative phosphorylation and RELMα expression (**Fig. 7b**,**c**) were all significantly greater in mice responding to the secondary infection. This correlated with resistance to secondary infection, apparent as an over 50% lower adult worm burden arising from secondary infection than from primary infection (**Fig. 7d**). We then sought to determine whether inhibition of lipolysis following secondary infection affected enhanced M2 activation or resistance to secondary infection. We found that treatment with orlistat prevented the increase in the number of peritoneal macrophages that occurred during secondary infection (**Fig. 7a**), inhibited all measured parameters of enhanced M2 activation (**Fig. 7b**,**c**) and suppressed the resistance to reinfection in immune mice (**Fig. 7d**).

Given the experimental approach used here, there was a possibility that orlistat was affecting not only macrophage function but also adaptive immunity. To address this, we used 4get/KN2 IL-4 reporter mice to quantify CD4$^+$ type 2 helper T cells (T_H2 cells) in mesenteric lymph nodes following primary or secondary infection with or without orlistat treatment. We found that inhibition of lipolysis during the development of the effector or secondary effector response had no measurable effect on the adaptive response, as assessed by the overall cellularity of the mesenteric lymph nodes (**Supplementary Fig. 6a**) and the number of IL-4-secreting T_H2 cells in the mesenteric lymph nodes (**Supplementary Fig. 6b**). Furthermore, examining IL-4 reporter expression in all live cells from mice treated with orlistat did not reveal any effects on non-T_H2 cell sources of IL-4 (data not shown). In summary, our data showed that inhibition of lipolysis was able to block the M2 activation of macrophages associated with resistance to the helminth parasite *H. polygyrus* and in so doing suppressed immunity to this pathogen.

DISCUSSION

We have shown that the enhanced FAO and related SRC in macrophages stimulated with IL-4 were dependent on a pathway of cell-intrinsic lipolysis mediated by the lysosomal enzyme LAL. Consistent with the necessity of generating fatty acids to fuel FAO and the importance of FAO for M2 activation, we found higher expression of LAL in M2 macrophages than in M1 macrophages and that this was critical for full M2 activation of macrophages in response to IL-4.

Mutations in the gene encoding LAL cause Wolman's disease and cholesterol ester–storage disease, which are characterized by varying degrees of accumulation of triacylglycerols and cholesterol esters not only in the liver, intestine and adrenal glands but also in the blood vessels and spleen. Notably, the accumulation of triacylglycerol in macrophages is associated with deficiencies in LAL activity, and atherosclerosis, a disease ameliorated by M2 activation[32,33], develops prematurely in cholesterol ester–`storage disease[25]. Moreover, genome-wide association studies have revealed that polymorphisms in *LIPA* are associated with premature human coronary artery disease with least three distinct genetic backgrounds[34,35]. Thus, a genetic link exists between LAL and a disease in which M2 macrophages are considered to have an important protective role. The clinical evidence provides support for the possibility that LAL has an important role in the biology of M2 macrophages. *Lipa*$^{-/-}$ mice represent a model of human LAL deficiencies and have provided insight into the role of LAL in the immune system. In these mice, which die prematurely, lymphopoiesis is diminished and is accompanied by a myeloproliferative disorder and multiorgan sterile inflammation[36] that can be reversed by the macrophage-specific expression of human LAL[37]; this supports the view that macrophage LAL has a critical role in the homeostatic control of inflammation. Such data are consistent with our finding that LAL was essential for M2 activation and the known ability of M2 activation to ameliorate inflammation in many settings. Notably, bone marrow transplantation has been used to treat Wolman's disease[38], which supports the view that lack of LAL expression in cells of hematopoietic origin is critical for the pathogenesis of this disease.

It has been suggested that compared with M1 macrophages, which exert their functions over short time periods, M2 macrophages are engaged in activities that are more prolonged, and that the relative efficiency of FAO versus that of glycolysis is well suited to meet the metabolic requirements of these roles[7]. Consistent with this view, we found that M2 macrophages survived longer than M1 macrophages did in culture and had substantial SRC, a characteristic that in CD8$^+$ T lymphocytes is linked to the enhanced FAO and cellular longevity of memory cells[10]. In parallel studies, LAL has also been found to be responsible for the generation of fatty acids for FAO in memory CD8$^+$ T cells, a process that is driven by IL-15 (ref. 39), which suggests

that LAL has broadly assumed the role of coordinating increases in FAO induced by cytokines (IL-4 or IL-15) to support the longevity of cells of the immune system. Notably, the population expansion of M2 peritoneal macrophages that occurred in immune mice following challenge infection with *H. polygyrus* did not occur when lipolysis was inhibited. This finding may reflect reduced survival of these cells due to diminished FAO, as was apparent in orlistat-treated M2 macrophages in tissue culture. An alternative explanation is that this failure was the result of reduced proliferation of the M2 macrophage population. Reports have indicated that helminth infection–induced M2 macrophages proliferate *in situ* and that population expansion in these cases is driven by proliferation rather than by the recruitment and differentiation of monocytes[23,30]. Thus, in addition to blocking the expression of genes encoding molecules associated with M2 activation, inhibition of lipolysis may also effectively block IL-4-induced macrophage proliferation, especially since fatty acids derived from the lipolysis of triacylglycerols can serve as building blocks for the synthesis of membrane lipids, which is critical in cells undergoing division. The lipolysis of triacylglycerols may also generate fatty acids that can serve as ligands for nuclear receptors such a PPARs, which regulate the expression of genes encoding molecules used for FAO and are critical for M2 activation[40]. It is feasible that inhibition of lipolysis influences macrophage fate following exposure to IL-4 by blocking these processes.

A published report has shown that IL-4 induces increased lipolysis in adipocytes by promoting hormone-sensitive lipase activity[41]. Nevertheless, we found that M2 activation associated with increased oxidative phosphorylation occurred normally in macrophages deficient in either ATGL or hormone-sensitive lipase (data not shown), which indicated that these cells used alternative pathways of lipolysis to liberate fatty acids from triacylglycerols. Our data showed that this alternative pathway was mediated by LAL, whose expression we found was higher in M2 macrophages and which has also been reported to have higher expression in human M2 macrophages than in M1 macrophages[28]. Notably, genes encoding lysosomal proteins show enrichment for STAT6 binding, as assessed by chromatin immunoprecipitation[42], which indicates that IL-4 generally induces lysosomal function. Our data provide support for the proposal that lysosomal lipolysis of triacylglycerols is critical for optimal M2 activation and link the uptake of triacylglycerol-carrying proteins such as VLDL and LDL through CD36 to this process. Notably, we found that IL-4-induced increases in oxidative phosphorylation and expression of CD206, CD301, PD-L2 and RELMα were unaffected by deletion of *Ldlr* itself (data not shown). Reports have indicated that the uptake of oxidized LDL via CD36 and platelet-activating factor receptor[43], as well as expression of the gene encoding the LDLR-related protein LRP1 (ref. 44), are sufficient to promote IL-4-independent expression of certain genes linked to the M2 phenotype, although the mechanisms underlying these effects are unclear. Moreover, the neutral cholesterol esterase hydrolases encoded by *Nceh1* and *Ces1g* have been linked to the ability of macrophages to serve an anti-inflammatory role in atherosclerosis[45,46], and expression of both of these genes, as well as of *Lrp1*, was somewhat elevated after stimulation with IL-4.

Our findings suggest that in addition to fueling FAO through the lipolysis of exogenous triacylglycerols, M2 macrophages can utilize endogenous triacylglycerols, generated from newly synthesized fatty acids, for the same purpose. We believe that these endogenously synthesized triacylglycerols contributed to the formation of lipid droplets in M2 cells in which lipolysis had been inhibited. On balance, the data indicate that the lipolysis of endogenously synthesized triacylglycerols is also mediated by LAL, since suppression of LAL expression in M2 cells also resulted in the accumulation of lipid droplets. It is unclear at present how LAL gains access to lipid droplets in M2 macrophages. In other non-adipocyte cells, lysosome-dependent autophagy has been reported to be important for the lipolysis of triacylglycerols in lipid droplets[47,48]. We have not found evidence to support the existence of this pathway in M2 macrophages cultured in complete medium (data not shown), but it is feasible that autophagy programs are engaged when access to fatty acids from exogenous triacylglycerols is restricted. However, autophagy-independent lysosomal lipolysis of lipid droplets by macrophages is not unprecedented[49], so it remains feasible that the lipolysis of endogenously synthesized triacylglycerols occurs through as-yet-unknown mechanisms.

M2 macrophages have important roles in immune responses to helminth parasites, acting to directly affect parasite health and persistence in sites of infection and/or to regulate T cell responses and associated immunopathology. Through the use of two models of elimination of the intestinal helminth parasite *H. polygyrus* by the immune system, we found that inhibition of lipolysis significantly diminished antiparasitic immunity promoted by the injection of IL-4 into mice carrying a primary infection and inhibited resistance to secondary infection in mice challenged after a drug-induced cure of the primary infection. In both cases, reductions in immunity were tightly correlated with decreases in oxidative phosphorylation and the expression of M2 markers in peritoneal macrophages. We found no evidence of an effect of inhibiting lipolysis on T_H2 cell responses, which indicated that the observed differences in immunity were probably not linked to reductions in the production of type 2 effector cytokines by the adaptive response, although we have not formally ruled out the possibility of an effect on other sources of IL-4 or IL-13. We infer from these findings that lipolysis has a role in M2 activation *in vivo* in the setting of helminth infection. There have been no reports to our knowledge of a role for LAL in immunity to parasitic helminths in mice or humans, but the latter may reflect the relative lack of genome-wide association studies to identify quantitative trait loci encoding molecules that affect human resistance to helminth parasites. Collectively, our data indicate that macrophages use the lysosomal pathway to mobilize fatty acids to facilitate FAO and the M2 activation program. Our findings suggest that approaches for gain or loss of function of LAL may offer therapeutic potential in diseases in which M2 macrophages have protective or detrimental effects.

METHODS

Methods and any associated references are available in the online version of the paper.

Accession codes. GEO: RNA-seq data set, GSE53053.

Note: Any Supplementary Information and Source Data files are available in the online version of the paper.

ACKNOWLEDGMENTS

We thank G. Haemmerle and R. Zechner for permission to use *Pnpla2*$^{-/-}$ mice; C. Semenkovich (Washington University in St. Louis) and R. Gross (Washington University in St. Louis) for *Pnpla2*$^{-/-}$ mice; H. Virgin, E.L. Gautier and S. Ivanov for discussions; and the staff of the Department of Pathology & Immunology Flow Cytometry Core and the Metabolomics Core of the Diabetic Cardiovascular Disease Center for technical assistance. Supported by the US National Institutes of Health (AI32573 and CA164062 to E.J.P.; AI091965 and CA158823 to E.L.P.; DK060022 to N.A.A.; HL087001 to H.D.; and CA138759 and CA152099 to C.Y.).

AUTHOR CONTRIBUTIONS

S.C.-C.H., B.E., Y.I., D.O., M.N., N.A.A., J.F.U., M.N.A., E.L.P. and E.J.P., designed experiments; S.C.-C.H., B.E., Y.I., D.O., M.N., A.M.S., W.B., L.L.-G., W.Y.L.,

C.M.O., C.Y. and H.D. did experiments; S.C.-C.H., B.E., M.N., D.O., W.Y.L., C.M.O., N.A.A., M.N.A., E.L.P. and E.J.P. analyzed data; and S.C.-C.H. and E.J.P. wrote the paper.

COMPETING FINANCIAL INTERESTS

The authors declare no competing financial interests.

1. Geissmann, F. *et al.* Development of monocytes, macrophages, and dendritic cells. *Science* **327**, 656–661 (2010).
2. Schulz, C. *et al.* A lineage of myeloid cells independent of Myb and hematopoietic stem cells. *Science* **336**, 86–90 (2012).
3. Gause, W.C., Wynn, T.A. & Allen, J.E. Type 2 immunity and wound healing: evolutionary refinement of adaptive immunity by helminths. *Nat. Rev. Immunol.* **13**, 607–614 (2013).
4. Gordon, S. Alternative activation of macrophages. *Nat. Rev. Immunol.* **3**, 23–35 (2003).
5. Wynn, T.A., Chawla, A. & Pollard, J.W. Macrophage biology in development, homeostasis and disease. *Nature* **496**, 445–455 (2013).
6. Rodríguez-Prados, J.C. *et al.* Substrate fate in activated macrophages: a comparison between innate, classic, and alternative activation. *J. Immunol.* **185**, 605–614 (2010).
7. Odegaard, J.I. & Chawla, A. Alternative macrophage activation and metabolism. *Annu. Rev. Pathol.* **6**, 275–297 (2011).
8. Vats, D. *et al.* Oxidative metabolism and PGC-1β attenuate macrophage-mediated inflammation. *Cell Metab.* **4**, 13–24 (2006).
9. Pearce, E.L. Metabolism in T cell activation and differentiation. *Curr. Opin. Immunol.* **22**, 314–320 (2010).
10. van der Windt, G.J. *et al.* Mitochondrial respiratory capacity is a critical regulator of CD8+ T cell memory development. *Immunity* **36**, 68–78 (2012).
11. Zechner, R. *et al.* FAT SIGNALS–lipases and lipolysis in lipid metabolism and signaling. *Cell Metab.* **15**, 279–291 (2012).
12. Kienesberger, P.C., Pulinilkunnil, T., Nagendran, J. & Dyck, J.R. Myocardial triacylglycerol metabolism. *J. Mol. Cell. Cardiol.* **55**, 101–110 (2013).
13. Su, X. & Abumrad, N.A. Cellular fatty acid uptake: a pathway under construction. *Trends Endocrinol. Metab.* **20**, 72–77 (2009).
14. Bharadwaj, K.G. *et al.* Chylomicron- and VLDL-derived lipids enter the heart through different pathways: *in vivo* evidence for receptor- and non-receptor-mediated fatty acid uptake. *J. Biol. Chem.* **285**, 37976–37986 (2010).
15. Feng, J. *et al.* Induction of CD36 expression by oxidized LDL and IL-4 by a common signaling pathway dependent on protein kinase C and PPAR-γ. *J. Lipid Res.* **41**, 688–696 (2000).
16. Oh, J. *et al.* Endoplasmic reticulum stress controls M2 macrophage differentiation and foam cell formation. *J. Biol. Chem.* **287**, 11629–11641 (2012).
17. Ries, S. *et al.* Transcriptional regulation of lysosomal acid lipase in differentiating monocytes is mediated by transcription factors Sp1 and AP-2. *J. Lipid Res.* **39**, 2125–2134 (1998).
18. Nicholls, D.G. *et al.* Bioenergetic profile experiment using C2C12 myoblast cells. *J. Vis. Exp.* **46**, e2511 (2010).
19. O'Neill, L.A. & Hardie, D.G. Metabolism of inflammation limited by AMPK and pseudo-starvation. *Nature* **493**, 346–355 (2013).
20. Thomas, G.D. *et al.* The biology of nematode- and IL4Ralpha-dependent murine macrophage polarization *in vivo* as defined by RNA-Seq and targeted lipidomics. *Blood* **120**, e93–e104 (2012).
21. Heck, A.M., Yanovski, J.A. & Calis, K.A. Orlistat, a new lipase inhibitor for the management of obesity. *Pharmacotherapy* **20**, 270–279 (2000).
22. Schweiger, M. *et al.* Adipose triglyceride lipase and hormone-sensitive lipase are the major enzymes in adipose tissue triacylglycerol catabolism. *J. Biol. Chem.* **281**, 40236–40241 (2006).
23. Jenkins, S.J. *et al.* Local macrophage proliferation, rather than recruitment from the blood, is a signature of TH2 inflammation. *Science* **332**, 1284–1288 (2011).
24. McLaren, J.E., Michael, D.R., Ashlin, T.G. & Ramji, D.P. Cytokines, macrophage lipid metabolism and foam cells: implications for cardiovascular disease therapy. *Prog. Lipid Res.* **50**, 331–347 (2011).
25. Sheriff, S., Du, H. & Grabowski, G.A. Characterization of lysosomal acid lipase by site-directed mutagenesis and heterologous expression. *J. Biol. Chem.* **270**, 27766–27772 (1995).
26. Hadváry, P., Sidler, W., Meister, W., Vetter, W. & Wolfer, H. The lipase inhibitor tetrahydrolipstatin binds covalently to the putative active site serine of pancreatic lipase. *J. Biol. Chem.* **266**, 2021–2027 (1991).
27. Harmon, C.M., Luce, P., Beth, A.H. & Abumrad, N.A. Labeling of adipocyte membranes by sulfo-N-succinimidyl derivatives of long-chain fatty acids: inhibition of fatty acid transport. *J. Membr. Biol.* **121**, 261–268 (1991).
28. Martinez, F.O., Gordon, S., Locati, M. & Mantovani, A. Transcriptional profiling of the human monocyte-to-macrophage differentiation and polarization: new molecules and patterns of gene expression. *J. Immunol.* **177**, 7303–7311 (2006).
29. Reynolds, L.A., Filbey, K.J. & Maizels, R.M. Immunity to the model intestinal helminth parasite *Heligmosomoides polygyrus*. *Semin. Immunopathol.* **34**, 829–846 (2012).
30. Jenkins, S.J. *et al.* IL-4 directly signals tissue-resident macrophages to proliferate beyond homeostatic levels controlled by CSF-1. *J. Exp. Med.* **210**, 2477–2491 (2013).
31. Anthony, R.M. *et al.* Memory T_H2 cells induce alternatively activated macrophages to mediate protection against nematode parasites. *Nat. Med.* **12**, 955–960 (2006).
32. Cardilo-Reis, L. *et al.* Interleukin-13 protects from atherosclerosis and modulates plaque composition by skewing the macrophage phenotype. *EMBO Mol. Med.* **4**, 1072–1086 (2012).
33. Stöhr, R. & Federici, M. Insulin resistance and atherosclerosis: convergence between metabolic pathways and inflammatory nodes. *Biochem. J.* **454**, 1–11 (2013).
34. Wild, P.S. *et al.* A genome-wide association study identifies LIPA as a susceptibility gene for coronary artery disease. *Circ. Cardiovasc. Genet.* **4**, 403–412 (2011).
35. Vargas-Alarcón, G. *et al.* Single nucleotide polymorphisms within LIPA (lysosomal acid lipase A) gene areassociated with susceptibility to premature coronary artery disease. A replication in the genetic of atherosclerotic disease (GEA) Mexican Study. *PLoS ONE* **8**, e74703 (2013).
36. Du, H. *et al.* Lysosomal acid lipase-deficient mice: depletion of white and brown fat, severe hepatosplenomegaly, and shortened life span. *J. Lipid Res.* **42**, 489–500 (2001).
37. Yan, C. *et al.* Macrophage-specific expression of human lysosomal acid lipase corrects inflammation and pathogenic phenotypes in lal–/– mice. *Am. J. Pathol.* **169**, 916–926 (2006).
38. Tolar, J. *et al.* Long-term metabolic, endocrine, and neuropsychological outcome of hematopoietic cell transplantation for Wolman disease. *Bone Marrow Transplant.* **43**, 21–27 (2009).
39. O'Sullivan, D. *et al.* Memory $CD8^+$ T cells use cell intrinsic lipolysis to support the metabolic programming necessary for development. *Immunity* **41**, 75–88 (2014).
40. Chawla, A. Control of macrophage activation and function by PPARs. *Circ. Res.* **106**, 1559–1569 (2010).
41. Tsao, C.H., Shiau, M.Y., Chuang, P.H., Chang, Y.H. & Hwang, J. Interleukin-4 Regulates lipid metabolism by inhibiting adipogenesis and promoting lipolysis. *J. Lipid Res.* **55**, 385–397 (2014).
42. Brignull, L.M. *et al.* Reprogramming of lysosomal gene expression by interleukin-4 and Stat6. *BMC Genomics* **14**, 853 (2013).
43. Rios, F.J. *et al.* Oxidized LDL induces alternative macrophage phenotype through activation of CD36 and PAFR. *Mediators Inflamm.* **2013**, 198193 (2013).
44. May, P., Bock, H.H. & Nofer, J.R. Low density receptor-related protein 1 (LRP1) promotes anti-inflammatory phenotype in murine macrophages. *Cell Tissue Res.* **354**, 887–889 (2013).
45. Bie, J., Zhao, B. & Ghosh, S. Atherosclerotic lesion progression is attenuated by reconstitution with bone marrow from macrophage-specific cholesteryl ester hydrolase transgenic mice. *Am. J. Physiol. Regul. Integr. Comp. Physiol.* **301**, R967–R974 (2011).
46. Sekiya, M. *et al.* Ablation of neutral cholesterol ester hydrolase 1 accelerates atherosclerosis. *Cell Metab.* **10**, 219–228 (2009).
47. Ouimet, M. *et al.* Autophagy regulates cholesterol efflux from macrophage foam cells via lysosomal acid lipase. *Cell Metab.* **13**, 655–667 (2011).
48. Singh, R. *et al.* Autophagy regulates lipid metabolism. *Nature* **458**, 1131–1135 (2009).
49. Xu, X.Y. *et al.* Obesity activates a program of lysosomal-dependent lipid metabolism in adipose tissue macrophages independently of classic activation. *Cell Metab.* **18**, 816–830 (2013).

ONLINE METHODS

Animals and *in vivo* experiments. C57BL/6J mice, 4get/KN2 mice, C57BL/6 *Cd36*$^{-/-}$ mice and B6.129P2-*Pnpla2tm*^{1Rze}/J (*Pnpla2*$^{-/-}$) mice were bred and maintained in specific pathogen–free conditions under protocols approved by the institutional animal care committee at Washington University School of Medicine and were used at 8–12 weeks of age. *Lipa*$^{+/+}$ and *Lipa*$^{-/-}$ mice were maintained at Indiana State University under specific pathogen–free conditions. In some experiments, mice were given intraperitoneal injection of tetrahydrolipistatin (orlistat; 200 mg per kg body weight; Cayman Chemical) or with 300 µl of 3% thioglycollate (Sigma) immediately before IL-4 in complex with mAb to IL-4 (IL-4c; containing 5 µg IL-4 (PeproTech) and 25 µg anti-IL-4 (11B11; BioXcell))[50]. For infection with *H. polygyrus bakeri*, we followed protocols described in detail[51]. Mice were infected by oral gavage with 200 infective L3 stage larvae. For secondary infection experiments, adult *H. polygyrus* were eliminated from infected mice by oral administration of pyrantel pamoate (1 mg per mouse; Columbia Laboratory) at day 14 after primary infection, and >5 weeks later the mice were 'challenge infected' with 200 L3 stage larvae by oral gavage. At day 9 after the challenge infection, mice were killed and parasite burdens were measured. For quantification of worms, intestines were removed and opened longitudinally and then were incubated for 4 h at 37 °C in a metal strainer on top of a 50-ml tube filled with phosphate-buffered saline (PBS; Corning). Parasites dropped through the filter into the tube and were recovered to be counted on a dissecting microscope. For quantification of parasite eggs, feces were collected from individual mice, then eggs were floated on saturated sodium chloride, collected and counted under a microscope.

Isolation of cells from mice. After naive or infected mice were killed, peritoneal exudate cells (PECs) were harvested by peritoneal lavage with sterile PBS containing 5% FBS (HyClone) at a volume of 10 ml per mouse. Total peritoneal exudate cells and peritoneal macrophages were quantified by being counted in combination with multicolor flow cytometry. For analysis of lymphocyte activation by flow cytometry, single-cell suspensions were prepared from lymphoid organs that had been forced through 70-µm strainers and washed with RPMI medium containing 5% FBS (Corning). Red blood cells were lysed with ACK lysis buffer (0.15 M NH_4Cl, 1 mM $KHCO_3$ and 0.1 mM EDTA). Bone marrow was flushed from the femur and tibia with RPMI medium containing 5% FBS and was dissociated into single-cell suspensions by repeated pipetting. Cells were maintained on ice until use or analysis.

Preparation of macrophages from bone marrow and macrophage activation. Bone marrow cells were differentiated for 7 d in the presence of recombinant mouse macrophage colony-stimulating factor (M-CSF; 20 ng/ml; R&D Systems) in complete medium (RPMI-1640 medium containing 10 mM glucose, 2 mM L-glutamine, 100 U/ml of penicillin-streptomycin and 10% FBS). Macrophages at day 7 were washed and then were stimulated for 24 h with various combinations of IL-4 (20 ng/ml; PeproTech) or lipopolysaccharide (20 ng/ml; Sigma) plus IFN-γ (50 ng/ml; R&D Systems) in the presence or absence of 200 µM etomoxir (Sigma), 20 µM SSO, 30 µM chloroquine (Sigma), 0.1 µM bafilomycin A1 (Tocris Bioscience), 100 µM orlistat (Cayman), 20 µM TOFA (5-(tetradecyloxy)-2-furoic acid; Sigma), 5 or 50 µg/ml of LDL (Kalen Biomedical) and VLDL (Kalen Biomedical). Macrophages were then harvested and were analyzed by flow cytometry for expression of markers of M1 or M2 activation. In some experiments, the survival of macrophages was monitored after M2 or M1 activation. For these experiments, bone marrow–derived macrophages (0.5×10^6 cells per well of a 48-well plate) were cultured in complete medium with mouse M-CSF (20 ng/ml) and were stimulated with IL-4 or LPS plus IFN-γ. Cell viability was monitored over time by flow cytometry of F4/80$^+$ cells stained with 7-amino-actinomycin D (BioLegend). Culture medium and stimulation reagents were replenished every 1 or 2 d.

Identification of human CD36-sufficient and CD36-deficient subjects. Venous blood samples were obtained from a CD36-deficient adult subject and an adult subject with normal CD36 expression, and peripheral blood mononuclear cells were isolated from he blood with Ficoll-Paque (GE Health Care) and density-gradient centrifugation. The CD36-deficient subject is homozygous for the G allele (allele frequency ~10%) of coding SNP rs3111938 (T/G), which introduces a stop codon and results in a truncated protein that is degraded. Homozygosity at the G allele results in complete CD36 deficiency[52]. The study was approved by the Washington University School of Medicine Institutional Review Board, and written informed consent was obtained from each subject.

Isolation of mononuclear cells from human peripheral blood and activation of human macrophages. Monocytes were purified from peripheral blood mononuclear cells with human CD14 MicroBeads (MACS) and then were differentiated into macrophages for 8 d in complete RPMI medium containing 20 ng/ml recombinant human M-CSF (R&D Systems). Human macrophages were harvested on day 8 and were stimulated for 24 h with 20 ng/ml human IL-4 (R&D Systems) or 50 ng/ml human IFN-γ (R&D Systems) plus 20 ng/ml LPS.

Retroviral transduction. Retroviral transduction of macrophages was accomplished with a protocol that we have used previously to transduce bone marrow–derived dendritic cells[53]. Sequence for shRNA targeting luciferase or *Lipa* was obtained from Open Biosystems andwas cloned into the retroviral vector MSCV-LTRmir30-PI8, which encodes human CD8 as a reporter. Two independent sequences were used to target *Lipa*: TCAAGTCCAGCATTCACTG and TGTGCTTCAGAGACCAGGT. Recombinant retroviruses were used for spin infection (800*g* for2 h) of bone marrow macrophage cultures at day 3. After 7 d in culture with M-CSF, macrophages were harvested and transduced macrophages were gated on the basis of human CD8 expression. Both shRNAs were used for experiments and produced similar results, but only data obtained with TGTGCTTCAGAGACCAGGT are presented here. For the bone marrow chimeras, bone marrow cells were collected from donor mice and were cultured for 24 h in complete RPMI medium containing 10 ng/ml IL-3, 10 ng/ml IL-6 and 50 ng/ml mouse c-Kit ligand. Cells were then transduced with retroviral shRNA targeting *Lipa* or luciferase, and 5×10^5 transduced cells were injected intravenously into irradiated recipients. Recipients were used 6–10 weeks later.

Treatment of peritoneal macrophages with siRNA. siRNA targeting mouse *Lipa* (AAAGCUAUGAAACCAUGGTg) was from Applied Biosystems, and Silencer Negative control siRNA#1, which does not match any sequence in the mouse genome, was also provided by the manufacturer and served as a control. siRNA (50 nM) was put into a complex with Lipofectamine 2000 and was delivered into peritoneal macrophages according to the manufacturer's instructions (Life Technologies). siRNA-treated peritoneal macrophages were then stimulated for 48 h with 20 ng/ml of IL-4 before analysis.

Metabolism assays. For real-time analysis of ECAR and OCR, macrophages were analyzed with an XF-96 Extracellular Flux Analyzer (Seahorse Bioscience) as described in detail for bone marrow–derived dendritic cells[53]. Three or more consecutive measurements were obtained under basal conditions and after the sequential addition of 1 µM oligomycin, to inhibit mitochondrial ATP synthase; 1.5 µM FCCP (fluoro-carbonyl cyanide phenylhydrazone), a protonophore that uncouples ATP synthesis from oxygen consumption by the electron-transport chain; and 100 nM rotenone plus 1 µM antimycin A, which inhibit the electron transport chain (all drugs for this assay from Sigma). In this assay, basal oxygen consumption can be established by measurement of OCR in the absence of drugs. Decreases in OCR after the addition of oligomycin and of rotenone and antimycin are expected and indicate that cells are consuming oxygen for mitochondrial oxidative phosphorylation. SRC is calculated as the difference between basal OCR and maximal OCR after the addition of FCCP. Maximal OCR occurs after the addition of FCCP, since cells attempt to maintain a proton gradient across the inner mitochondrial membrane by increasing the consumption of oxygen by the electron-transport chain[10,53]. Global metabolite profiling of stimulated macrophages was performed with mass spectrometry by Metabolon. Glycerol in macrophage supernatants was measured as absorbance at 570 nm after incubation with Free Glycerol Reagent (Sigma) and by comparison to a glycerol standard (Sigma). For lipidomic analysis, washed cell pellets were frozen and thawed and homogenized in 500 µl of PBS with an Omni Bead Ruptor 24 (Omni International): 50 µl of each homogenate was reserved for protein measurement; 450 µl of each homogenate was used for lipidomic analysis. A modified Bligh-Dyer extraction method

doi:10.1038/ni.2956

was used for extraction of lipids in the presence of an internal standard mixture. A Shimadzu 10A HPLC system coupled to a TSQ Quantum Ultra triple quadrupole mass spectrometer operated in SRM mode under ESI(+) was used for mass spectrometry. Different analytical HPLC columns and mobile phases were used for different analytes to achieve the optimal sensitivity and separation. A pooled lipid extract from study samples served for quality control and was injected between every sample for verification of instrument consistency, and is stated as 'percent CV of QC'. Only species with a 'percent CV of QC' value of <15% were reported. Data were processed with Xcalibur software (Thermo). The concentration of an analyte was calculated as the concentration of its corresponding internal standard multiplied by the peak area ratio of the analyte to the internal standard, based on the assumption that the MS responses of the analyte and internal standard are the same.

Flow cytometry. Cells were kept at 4 °C and nonspecific binding was blocked with 5 μg/ml of anti-CD16/32 (93; eBiosciences) before cell surfaces were stained with anti-CD11b (M1/70; eBiosciences), anti-F4/80 (BM8; eBiosciences), anti-CD206 (C068C2; Biolegend), anti-CD301 (ER-MP23; AbD Serotec), anti-PD-L2 (TY25; eBiosciences), anti-CD62L (MEL-14; BD Biosciences), anti-CD44 (IM7; BD Biosciences), anti-CD4 (RM4-5; BD Biosciences) and/or antibody to human CD2 (RPA-2.10; BD Biosciences). For intracellular staining of RELMα and iNOS, cells were fixed in 4% ultrapure paraformaldehyde and were stained for 1 h at 22 °C with rabbit anti-RELMα (500-P214; PeproTech) and mouse anti-Nos2 (C-11; Santa Cruz Biotechnology) in 0.2% saponin buffer, followed by incubation with the appropriate fluorochrome-conjugated antibody to rabbit IgG (711-096-152; Jackson Immunoresearch) or antibody to mouse IgG (A85-1; BD Biosciences) in the same buffer. BODIPY-labeled LDL (10 μg/ml; Invitrogen), BODIPY-labeled VLDL (10 μg/ml; Kalen Biomedical) and BODIPY-labeled palmitate (1 μM; Invitrogen) were used in conjunction with flow cytometry for uptake experiments. Intracellular neutral lipids were stained with 500 ng/ml BODIPY 493/503 (Invitrogen) and fluorescence due to binding of BODIPY was measured by flow cytometry. All macrophage staining data presented here represent cells gated as $CD11b^+F4/80^+$, and all cells were living, as assessed by staining with LIVE/DEAD (Invitrogen) or 7-amino-actinomycin D (eBiosciences). Human macrophages were stained with anti–human CD14 (MϕPg; BD Biosciences), anti–human CD36 (CB38; BD Biosciences) and anti–human CD206 (15-2; Biolegend). Staining results are presented for $CD14^+$ cells. Data were acquired on a FACSCanto II (BD Biosciences) and were analyzed with FlowJo software version 9.5.2 (TreeStar).

RNA sequencing. Cells were stimulated for 24 h, then mRNA was extracted from lysates of the cells with oligo(dT) beads (Invitrogen). The synthesis, sequencing and sequence analysis of cDNA were done as described[54]. Raw and processed sequencing data were deposited at PubMed.

Transmission electron microscopy. For ultrastructural analysis, cells were fixed for 1 h at 22 °C in 2% paraformaldehyde, 2.5% glutaraldehyde (Polysciences) and 0.05% malachite green (Sigma) in 100 mM sodium cacodylate buffer, pH 7.2. The malachite green was incorporated into the fixative for stabilization of lipid constituents soluble in aqueous glutaraldehyde. Samples were washed in cacodylate buffer and were post-fixed for 1 h in 1% osmium tetroxide (Polysciences). Samples were then rinsed extensively in distilled H_2O before *en bloc* staining for 1 h with 1% aqueous uranyl acetate (Ted Pella). Following several rinses in distilled H_2O, samples were dehydrated in a graded series of ethanol and embedded in Eponate 12 resin (Ted Pella). Sections 95 nm in thickness were cut with a Leica Ultracut UC7 ultramicrotome (Leica Microsystems), then were stained with uranyl acetate and lead citrate and viewed on a JEOL 1200 EX transmission electron microscope (JEOL USA) equipped with an AMT eight-megapixel digital camera (Advanced Microscopy Techniques).

Statistical analysis. Data were analyzed with Graphpad Prism software (version 5). Comparisons of two groups were calculated by one-way ANOVA and, where indicated, with unpaired two-tailed Student's *t*-tests. Differences with *P* values below 0.05 were considered significant. No randomization or exclusion of data points was used. Pilot *in vivo* studies were used for estimation of the sample size required to ensure adequate power.

50. Finkelman, F.D. *et al.* Anti-cytokine antibodies as carrier proteins. Prolongation of *in vivo* effects of exogenous cytokines by injection of cytokine-anti-cytokine antibody complexes. *J. Immunol.* **151**, 1235–1244 (1993).
51. Camberis, M., Le Gros, G. & Urban, J. Jr. in *Current Protocols in Immunology* (ed. Coico, R.) Ch. 19, Unit 19 12 (Wiley, 2003).
52. Love-Gregory, L. *et al.* Common CD36 SNPs reduce protein expression and may contribute to a protective atherogenic profile. *Hum. Mol. Genet.* **20**, 193–201 (2011).
53. Krawczyk, C.M. *et al.* Toll-like receptor-induced changes in glycolytic metabolism regulate dendritic cell activation. *Blood* **115**, 4742–4749 (2010).
54. Sojka, D.K. *et al.* Tissue-resident natural killer cells are cell lineages distinct from thymic and conventional splenic NK cells. *eLife.* **3**, e01659 (2014).